Protein Science (1998), 7:2623–2630. Cambridge University Press. Printed in the USA.

Probing the ligand binding domain of the GluR2 receptor by proteolysis and deletion mutagenesis defines domain boundaries and yields a crystallizable construct

GUO-QIANG CHEN,[1] YU SUN,[1] RONGSHENG JIN, AND ERIC GOUAUX

Department of Biochemistry and Molecular Biophysics, Columbia University, 650 West 168th Street, New York, New York 10032

(RECEIVED July 15, 1998; ACCEPTED August 31, 1998)

Abstract

Ionotropic glutamate receptors constitute an important family of ligand-gated ion channels for which there is little biochemical or structural data. Here we probe the domain structure and boundaries of the ligand binding domain of the AMPA-sensitive GluR2 receptor by limited proteolysis and deletion mutagenesis. To identify the proteolytic fragments, Maldi mass spectrometry and N-terminal amino acid sequencing were employed. Trypsin digestion of HS1S2 (Chen GQ, Gouaux E. 1997. *Proc Natl Acad Sci USA 94*:13431–13436) in the presence and absence of glutamate showed that the ligand stabilized the S1 and S2 fragments against complete digestion. Using limited proteolysis and multiple sequence alignments of glutamate receptors as guides, nine constructs were made, folded, and screened for ligand binding activity. From this screen, the S1S2I construct proved to be trypsin- and chymotrypsin-resistant, stable to storage at 4 °C, and amenable to three-dimensional crystal formation. The HS1S2I variant was readily prepared on a large scale, the His tag was easily removed by trypsin, and crystals were produced that diffracted to beyond 1.5 Å resolution. These experiments, for the first time, pave the way to economical overproduction of the ligand binding domains of glutamate receptors and more accurately map the boundaries of the ligand binding domain.

Keywords: crystallization; glutamate receptor; ligand binding domain; mutagenesis; protease accessibility

Ionotropic glutamate receptors (iGluRs), located in the postsynaptic membrane, open transmembrane ion channels following the binding of agonist released from the presynaptic membrane (Seeburg, 1993; Hollmann & Heinemann, 1994; Nakanishi & Masu, 1994; Mori & Mishina, 1995; Wo & Oswald, 1995). Flux of monovalent and divalent cations through the postsynaptic membrane depolarizes the cell and propagates the electrical impulse (Hume et al., 1991; Verdoorn et al., 1991; Dingledine et al., 1992; Ferrer-Montiel et al., 1996). iGluRs can be divided into three subtypes based on their agonist binding properties: AMPA (α-amino-3-hydroxy-5-methylisoxazole-4-propionic acid) receptors are GluR1-4, NMDA (N-methyl-D-aspartate) receptors include NMDAR1 and NMDAR2a-d, and KA (kainate) receptors are composed of GluR5-7 and KA1-2 (Watkins et al., 1990; Hollmann & Heinemann, 1994). Electrophysiological studies have suggested that the ligand-gated, cation-permeable channel is a tetrameric complex (Laube et al., 1998; Mano & Teichberg, 1998; Rosenmund et al., 1998). Each subunit (Fig. 1A) has a ca. 400 residue N-terminal domain, a ligand binding domain (S1 and S2; O'Hara et al., 1993; Stern-Bach et al., 1994; Kuusinen et al., 1995), three transmembrane segments (M1, M3, and M4), and a membrane-embedded reentrant loop (M2; Hollmann et al., 1994; Wo & Oswald, 1994; Bennett & Dingledine, 1995).

Salient features of the iGluR ligand binding domain have been defined by comparison with the bacterial periplasmic ligand binding proteins (Nakanishi et al., 1990; Tam & Saier, 1993), by mutagenesis (O'Hara et al., 1993; Kuryatov et al., 1994; Mano et al., 1996; Paas et al., 1996; Wo & Oswald, 1996), by chimera (Stern-Bach et al., 1994), and by S1-S2 fusion experiments (Kuusinen et al., 1995; Arvola & Keinänen, 1996). Recently, large-scale production of the HS1S2 ligand binding domain (Fig. 1B) was achieved by *Escherichia coli* expression and in vitro folding (Chen & Gouaux, 1997). However, further investigation showed that the HS1S2 construct was protease-sensitive and unstable at room temperature. Therefore, we focused on more accurate delineation of the ligand binding domain boundaries and construction of more stable variants for biochemical and structural studies. These aims were ac-

Reprint request to: Eric Gouaux, Department of Biochemistry and Molecular Biophysics, Columbia University, 650 West 168th Street, New York, New York 10032; e-mail: jeg52@columbia.edu.

[1] These authors made equal contributions to the research reported here.

Abbreviations: iGluR, ionotropic glutamate receptor; GluR2, the iGluR subtype 2 or B; HS1S2, a recombinant ligand binding domain of GluR2, for a detailed definition of constructs HS1S2X, where X = A, B, C, D, E, F, G, H, I, J, see Figure 1B; S1S2X, HS1S2X without the His tag; pHS1S2X, plasmid with the gene coding for HS1S2X; AMPA, α-amino-3-hydroxy-5-methylisoxazole-4-propionic acid; NMDA, N-methyl-D-aspartate; Maldi-MS, matrix-assisted laser desorption/ionization-mass spectrometry; SEC, size exclusion chromatography; SeMet S1S2I, the selenomethionine derivative of S1S2I; GSH, reduced glutathione; GSSG, oxidized glutathione.

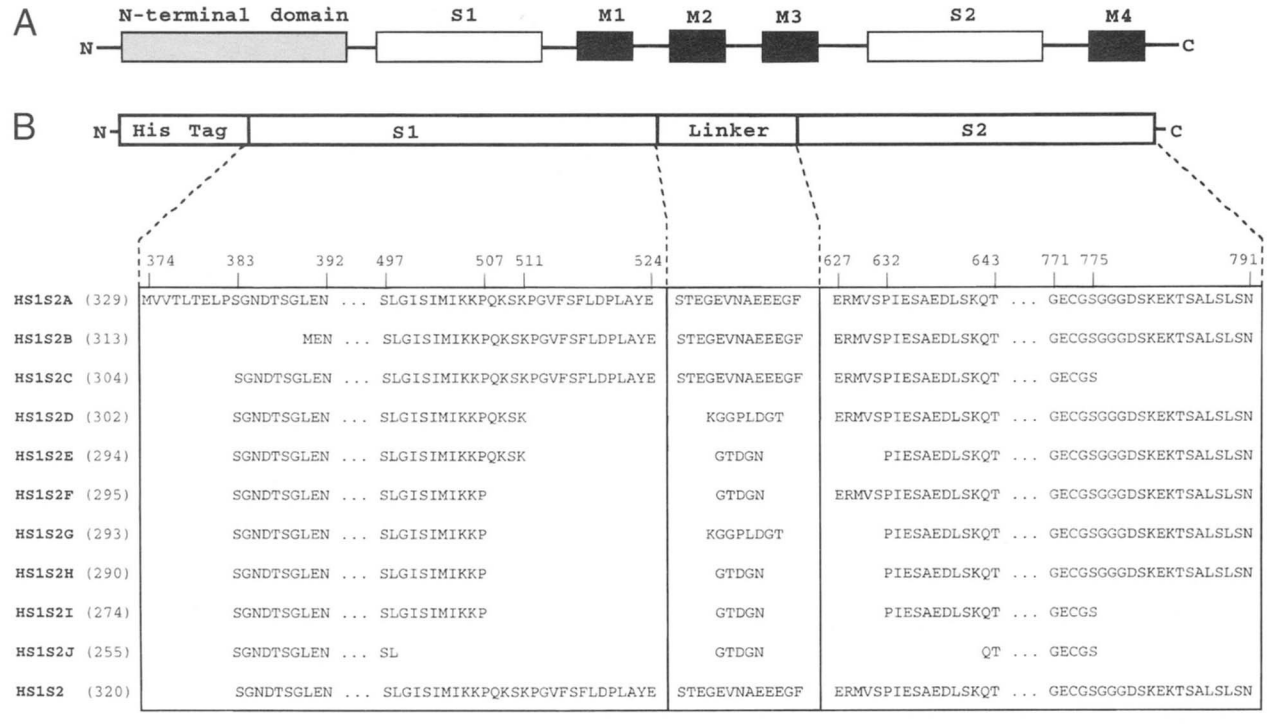

Fig. 1. Schematic representation of the (**A**) full length and (**B**) shortened constructs of the recombinant ligand binding domain of the rat GluR2. The ligand binding domain is composed of S1 and S2 segments, which are separated by transmembrane segments M1, M2, and M3 in the full length receptor but which are joined with a linker in the recombinant constructs discussed here. The His tag sequence is MHHHHHHHHSSGLVPR. Between the His tag and the start of S1 is the sequence GSAMG. The numbers after the construct names represent the total number of amino acid residues.

complished by limited proteolysis and subsequent Maldi-MS analysis (matrix-assisted laser desorption/ionization-mass spectrometry; Cohen et al., 1995; Cohen, 1996), N-terminal sequence analysis, and deletion mutagenesis of the HS1S2 construct. Deletion of the sequences peripheral to the ligand binding domain resulted in a construct that was biologically active and protease-resistant, as well as more thermally stable and crystallizable than longer constructs.

Results

Glutamate stabilizes the ligand binding domain against digestion by trypsin

Glutamate (1 mM) significantly stabilized the major proteolytic fragments in the trypsin digestion reaction mixture of HS1S2 (Fig. 2). Maldi-MS showed that the fragment at 17,780 corresponded to the sequence GSAMGS383-R628 and the peak at m/z 17,143.6 to M629-K783. The His tag (MHHHHHHHHSSGLVPR) cleaved from the N-terminus of HS1S2 at the thrombin site was detected at m/z 1,944.79. Additional fragments were most likely derived from further digestion of the major fragments. For example, the fragment at m/z 16,888.8 (M629-K781) may be derived from fragment M629-K783 by cleavage of the two C-terminal residues (EK). Cleavage at R661 of fragment M629-K783 resulted in fragments M629-R661 at m/z 3,696.75 and S662-K783 at m/z 8,684.28. The fragment at m/z 3,337.28 (S510-R628) may be from further digestion of the GSAMGS383-R628 fragment. The Maldi-MS data of the chymotrypsin digestion showed that cleavage at sites Y405, F491, Y523, and F667 gave relatively large fragments. Selected peaks and corresponding sequences are as follows: m/z 19,307.1, V406-F667; m/z 9,658.06, S492-F667; m/z 3,907.8, E524-Y647; m/z 2,007.65, V406-Y421; m/z 1,828.35, E422-F438; m/z 1,289.6, G648-F659.

Folding of HS1S2 deletion mutants

Variants of HS1S2 with deletions at the S1 and S2 termini and with different linkers (Fig. 1B) were prepared to test whether these

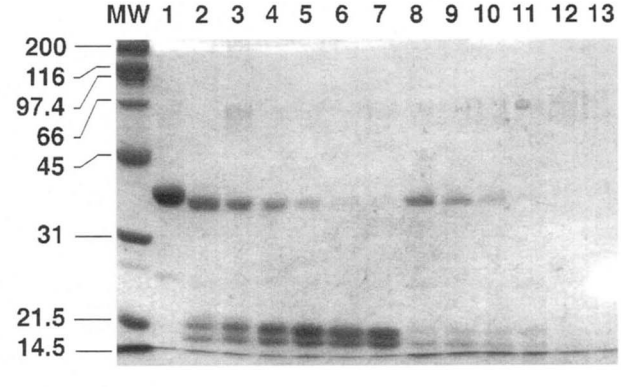

Fig. 2. Trypsin digestion of HS1S2 in the presence and absence of glutamate. Lane 1, no enzyme; lanes 2–7 correspond to digestion times 5, 10, 20, 30, 45, and 60 min with glutamate (2 mM), respectively; lanes 8–13 are the same as lanes 2–7 except that there was no glutamate present in the reaction.

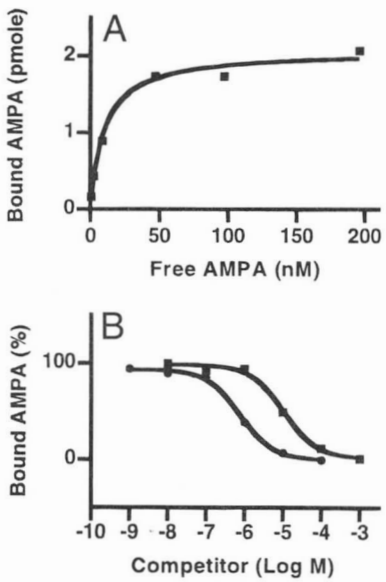

Fig. 3. HS1S2I ligand binding properties. **A:** [^{3}H]-AMPA saturation binding. **B**: Competition by glutamate (circles) and kainate (squares) for [^{3}H]-AMPA.

deletions and the linker length affect folding, stability, and ligand binding activity. All of the mutants except HS1S2B were overexpressed in BL21(DE3) cells at a similar level to HS1S2, were solubilized in Buffer 7 and were purified by size exclusion chromatography (SEC) in Buffer 8 to about 95% purity. On the basis of the behavior of HS1S2 in our folding screen (Chen & Gouaux, 1997), the optimized conditions were selected to examine the folding of the mutants. After folding using condition 2 (Chen & Gouaux, 1997), the [^{3}H]-AMPA binding activity of all constructs, except for HS1S2J, was greater than 8,000 cpm. Nonspecific binding was typically below 100 cpm. The HS1S2J construct, when subjected to multiple folding conditions that yielded species with high [^{3}H]-AMPA binding activity for the other constructs, did not bind [^{3}H]-AMPA. The HS1S2I [^{3}H]-AMPA saturation binding and the competition binding between [^{3}H]-AMPA and glutamate and kainate are illustrated in Figure 3. The K_d value for [^{3}H]-AMPA binding is 9.9 nM. The IC_{50} values for glutamate and kainate are 0.76 and 11 μM, respectively.

Optimization of HS1S2I folding by variations of pH, ionic strength, and concentrations of arginine and guanidine hydrochloride showed that folding in Buffer 9 produced a 30% yield of solubilized HS1S2I, as estimated by OD_{280} (1 mg/mL $\simeq$ 1.0 OD_{280}). At this stage, the solubilized protein was composed of monomeric and aggregated proteins. During concentration of the folding mixture, the percentage of monomer in the solution increased, probably due to precipitation of the aggregated material. After about 30-fold concentration of the HS1S2I folding reaction mixture, the percentage of monomeric HS1S2I was ~85% as analyzed by FPLC. The folded monomer was separated from the aggregate by SEC on a Superose 12 column. The precipitated protein was recycled twice. A total of 450 mg of purified monomeric HS1S2I was obtained from 10 L of *E. coli* culture.

S1S2I is a more stable and protease-resistant construct for crystallization

The thermal stability of S1S2I and S1S2 was analyzed by measuring the ligand binding activity after incubation of the protein at different temperatures. The ligand binding activity was 80 and 85% at 4 °C after 4 weeks, 0 and 50% at room temperature after 2 weeks, and 29 and 63% at 37 °C after 15 min for S1S2 and S1S2I in Buffer 4, respectively. These results demonstrated that S1S2I was more stable to thermal denaturation than S1S2. The protease accessibility of HS1S2I was analyzed by trypsin and chymotrypsin digestion and was compared to HS1S2 (Fig. 4). The S1S2 domain of HS1S2I was not digested by trypsin or chymotrypsin under conditions that fragmented HS1S2. The resistance of S1S2I to proteolysis may result from removal of the most accessible sites between the S1 and S2 regions and from reduction in flexibility and thus accessibility. The stability of S1S2I to trypsin facilitated the cleavage of the His tag from HS1S2I to give S1S2I for crystallization.

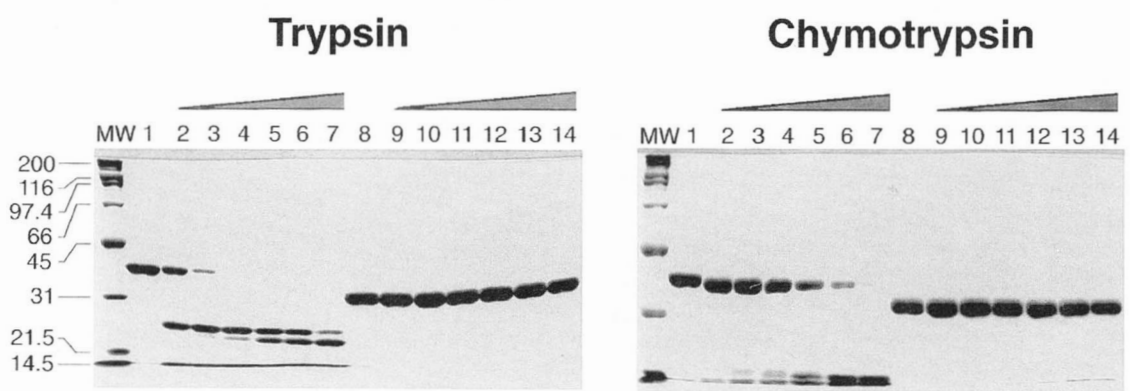

Fig. 4. Comparison of HS1S2 and HS1S2I by partial proteolysis. The reaction mixture was composed of 1.5 mg/mL protein and different protease concentrations in buffer 2 supplemented with 1 mM glutamate and 10 mM $CaCl_2$. The proteolysis reactions were carried out at room temperature for 40 min and stopped by addition of PMSF. Lanes 1–7 are HS1S2 reaction mixtures with protease/protein ratios of 0, 1/3,200, 1/1,600, 1/800, 1/400, 1/200, and 1/100 for trypsin (w/w), or 0, 1/80,000, 1/40,000, 1/20,000, 1/10,000, 1/5,000, and 1/2,500 for chymotrypsin (U/μg); lanes 8–14 are HS1S2I reactions performed under the same conditions as the reactions analyzed in lanes 1–7.

Crystallization of S1S2

Since S1S2 was not stable at or above room temperature, all crystallization experiments were carried out at 4 or 12 °C. The Hampton Crystal Screen Kit (catalog # HR2-110, Jancarik & Kim, 1991), the ammonium sulfate-pH Grid Screen Kit (catalog # HR2-211), and the MPD-pH Grid Screen Kit (catalog # HR2-215) did not give any crystals of S1S2 in the presence of glutamate. The PEG 6000-pH Grid Screen Kit (catalog # HR2-213) gave needles plus precipitate in the presence of 0.1 M HEPES, 10% PEG 6000, pH 7–9, 4 °C. Extensive screening of S1S2 in the presence of glutamate as a function of pH, PEG and different additives can be summarized as follows. (1) Crystals formed in a neutral to mildly basic pH range (pH 7–8.5). (2) The critical PEG concentrations in the reservoir were ~2.5% for PEG 12000, ~7.5% for PEG 6000, or ~15% for PEG 1000 and PEG 400 at a protein concentration of 10 mg/mL. (3) The following additives, employed separately, minimized protein precipitation and enhanced crystallization: 10–50 mM benzamidine chloride, 10–100 mM NDSB-256, 10–50 mM lithium sulfate, 10 mM ammonium sulfate, 10 mM potassium phosphate, or 50 mM arginine hydrochloride (Fig. 5A). (4) Only thin needle crystals were obtained from screening at 4 °C. Thicker needle crystals and rectangular bar crystals of glutamate-bound S1S2 were formed at 12 °C but not at 4 °C (Fig. 5B,C). However, no crystals of glutamate-bound S1S2 with the two small dimensions larger than 0.02 mm were obtained.

Kainate-bound S1S2 gave plate crystals under two conditions in the Hampton Crystal Screen Kit (Jancarik & Kim, 1991) and under one condition in the PEG 6000-pH Grid Screen Kit. These conditions were (1) 25% PEG 4000, 0.1 M NaOAc, pH 4.6, 0.2 M ammonium sulfate; (2) 30% PEG 4000, 0.2 M ammonium sulfate, pH 5.7; and (3) 20% PEG 6000, 0.1 M citric acid, pH 5.0. Further screening showed that low pH (pH 4.5–6.5) and PEG favored crystal formation. Although PEG 6000 (15–20%), 1000 (20–25%), or PEG MME 550 (18–30%) all produced nonneedle S1S2 crystals, the crystals (Fig. 5D, diffraction to 2.5 Å) obtained from the PEG 3350 solution were less multiple than those from other PEG solutions.

Crystallization of S1S2I

S1S2I crystallized much more readily than S1S2. For example, the crystallization screen of glutamate-bound S1S2I using the Hampton Crystal Screen Kit produced well-defined needles, similar to those shown in Figure 5A, under multiple conditions. Three of these conditions were (1) 0.2 M calcium acetate, 0.1 M sodium cacodylate, 18% PEG 8000, pH 6.5; (2) 0.1 M Tris-HCl, 8% PEG 8000, pH 8.5; and (3) 0.1 sodium HEPES, 10% 2-propanol, pH 7.5, 20% PEG 4000. Crystallization of kainate-bound S1S2I using the Hampton Crystal Screen Kit revealed a number of conditions that formed non-needle crystals: (1) 30% PEG 4000, 0.2 M ammonium sulfate, pH 5.7; (2) 20% PEG 8000, 0.05 M KH_2PO_4, pH 4.8, and (3) 30% PEG 1500. After optimization of the conditions employing kainate, well defined but small crystals (the largest dimension <0.05 mm, Fig. 5E) were obtained. The optimized conditions involved a series of buffers with 50 mM potassium phosphate, pH 4.0–5.5 and 11–16% PEG 8000. Small seed crystals (Fig. 5E) produced crystals with dimensions >0.2 mm (Fig. 5F) and which diffracted to 1.7 Å resolution at home using CuKα X-rays and to 1.5 Å using synchrotron radiation. Different crystal

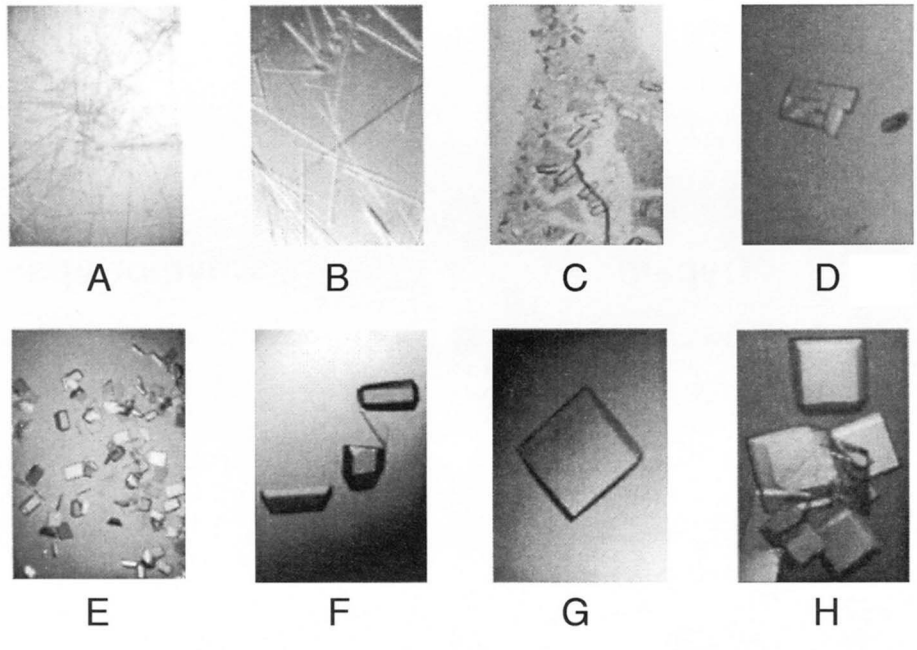

Fig. 5. Crystals of S1S2, S1S2I, and SeMet S1S2I. The conditions are defined as follows (protein + ligand, reservoir solution). (**A**) S1S2 + glutamate, 0.1 M HEPES, pH 8.0, 10% PEG 6K, 50 mM arginine-HCl; (**B**) S1S2 + glutamate, 0.1 M NaOAc, pH 6.0, 21% PEG 1K, 10 mM Li_2SO_4; (**C**) S1S2 + glutamate, 0.1 M NaOAc, pH 6.0, 22.5% PEG 1K, 50 mM Li_2SO_4; (**D**) S1S2 + kainate, 0.1 M NaOAc, pH 5.0, 21% PEG 3350, 200 mM $(NH_4)_2SO_4$; (**E**) S1S2I + kainate, 50 mM potassium phosphate, pH 4.0, 12% PEG 8K; (**F**) S1S2I + kainate, 50 mM potassium phosphate, pH 5.5, 13% PEG 8K; (**G**) SeMet S1S2I + kainate, 50 mM potassium phosphate, pH 5.0, 15% PEG 8K; (**H**) SeMet S1S2I + kainate, 50 mM potassium phosphate, pH 4.5, 15% PEG 8K.

morphologies were found under the same conditions as shown in Figure 5E and 5F. The SeMet S1S2I crystals (Fig. 5G,H) diffracted to 1.7 Å using synchrotron radiation and were obtained under conditions optimized for S1S2I supplemented with 1 mM DTT in the drop and well solution. The space group and unit cell dimensions of the S1S2I-kainate complex were $P2_1$ and $a = 43.22$ Å, $b = 63.07$ Å, $c = 46.32$ Å, and $b = 92.99°$. The methionine and selenomethionine crystals were isomorphous. On the basis of the mass of the S1S2I protein and the volume of the asymmetric unit, $Z = 2$.

Discussion

Large-scale production of functional recombinant proteins is a prerequisite for many biochemical, pharmaceutical, and structural studies. When substantial amounts of protein are not available from natural sources or when the native construct is not suitable for detailed investigations, an efficient heterologous expression and purification system for recombinant proteins is critical. Although iGluRs have been successfully expressed in Hela cells, *Xenopus oocytes*, baculovirus-infected insect cells (Bettler et al., 1990; Keinänen et al., 1994; Kuusinen et al., 1995) and in the periplasm of *E. coli* cells (Arvola & Keinänen, 1996), the amounts and the purity of protein are not suitable for extensive biochemical and structural studies. Here we show that overexpression of HS1S2 constructs in *E. coli* cells and efficient in vitro folding can yield large amounts of biologically active, thermally stable, protease-resistant, and homogenous GluR2 ligand binding domains for structure determination by X-ray crystallography.

As described here, 450 mg of folded and purified HS1S2I monomer were obtained from 10 L of *E. coli* culture. We took advantage of the initial in vitro folding conditions (Chen & Gouaux, 1997), which were subsequently improved by an additional fractional factorial screen. Dialysis of the denatured S1S2I solution at a protein concentration of 1–1.2 mg/mL against Buffer 9 resulted in a reproducible yield of 30% solubilized protein. When exploring methods to scale-up the HS1S2I folding reaction, we tried (1) to fold by dilution into a large volume and to recover the folded protein on a Ni^{2+} column and (2) to fold by slow and continuous dilution into a small volume dialysis chamber that was continuously dialyzed against folding buffer. Although the latter condition has not been optimized, it does provide a promising method because manipulation of large volumes is minimized. For example, by employing the latter method of continuous addition coupled to dialysis, the final concentration of folded HS1S2 reached 5 mg/mL.

Limited proteolysis combined with Maldi-MS techniques provided a powerful approach to probe the boundaries of the GluR2 ligand binding domain. Stabilization of the major proteolytic fragments by glutamate suggested that they were structurally associated and that their proteolytic susceptibility was related to ligand binding. The trypsin-sensitive sites were located at the thrombin site, K509, R628, and K783 and are among 44 potential trypsin sites. On the basis of the limited proteolysis data, we propose that the following sequences are not essential for ligand binding: (1) the His tag, (2) Q508-E524, (3) the linker, (4) E627-S631, and (5) G776-N791. The fact that S1S2I was more thermally stable and crystallizable than S1S2 was most likely due to the removal of flexible sequences that were nonessential for ligand binding. The conclusion that S1S2I is close to the minimum construct for ligand binding is based on the following results. (1) Multiple sequence alignment of GluR 1–7 revealed that N392 and V397-T399 at the N-terminus of S1, K506 and P507 at the C-terminus of S1, P632 and I633 at the N-terminus of S2 and K765-W767 at the C-terminus of S2 are conserved residues. These residues are close to the termini of S1 and S2 in the S1S2I construct (Fig. 1B). (2) The sizes of the S1 and S2 sequences in S1S2I were similar to the major proteolytic fragments in the trypsin digestion mixture of HS1S2 plus glutamate. Inspection of multiple sequence alignments of iGluRs and bacterial periplasmic amino acid binding proteins showed that the binding proteins do not have the sequences corresponding to Q508-E524, F623-E634, and W766-G791 of GluR2 (Sutcliffe et al., 1996). These "peripheral" regions correspond to the sequences that were readily digested in the limited proteolysis of HS1S2. (3) Deletion of Q508-E524, E627-S631, and G776-N791 by mutagenesis did not affect ligand binding activity while deletion of G499-P507 and P632-K641 abolished the binding activity. The similarity in folding properties and ligand binding activity between HS1S2I and the longer constructs combined with the inactivity of HS1S2J are consistent with the minimal ligand binding domain as defined by the proteolysis data. Other mutagenesis studies of GluR4 (or GluRD) showed that deletion of E628-A637, which corresponds to E627-A636 of GluR2, resulted in a decrease in AMPA binding activity, and deletion of I503-E525 (I502-E524 in GluR2) led to a total loss of ligand binding activity (Keinänen et al., 1998).

Increased stability of S1S2I compared to S1S2 may result from deletion of the flexible terminal sequences of S1 and S2 segments and the shortened linker. Based on the analogy with the bacterial periplasmic ligand binding proteins, we hypothesized that the residues entering and exiting the linker would adopt a β-strand conformation. The linkers used in the constructs of the GluR2 ligand binding domain reported here have the following features. They (1) form turns between β-strands in known structures determined at high resolution, (2) have different lengths, and (3) have a small number of glycines to provide flexibility while not disfavoring protein folding (Nagi & Regan, 1997). Specifically, the pentapeptide linker is a sequence from a 3:5 β-turn (Sibanda et al., 1989) in concanavalin A (Reeke et al., 1975) and the octapeptide sequence is from a 8:8 β-turn from carbonic anhydrase C (Liljas et al., 1972). The 13-residue linker is from the sequence that connects the immunoglobulin heavy chain to the hydrophobic transmembrane segment in the membrane-bound form of IgM (Rogers et al., 1980) and has been used to link the S1 and S2 segments of GluR4 and GluR2 (Arvola & Keinänen, 1996).

Protection of the entire S1S2I domain and the major proteolytic fragments of S1S2 by glutamate in the trypsin digestion reactions demonstrated that ligand binding stabilized the protein conformation. Possible stabilization of the protein conformation by ligand binding was also reflected in the significant difference in crystallization behavior between the ligand-free S1S2 and ligand-bound protein. Under the same crystallization conditions, S1S2 had a much higher tendency to precipitate in the absence of ligand than in the presence of glutamate, AMPA, or kainate. We speculate that precipitation under conditions with both high and low protein concentrations is probably due to protein denaturation and aggregation rather than to precipitation of folded monomeric species.

The crystallization behavior of the glutamate-bound S1S2 was very similar to that of the AMPA-bound S1S2, but very different from that of the kainate-bound protein. The most significant difference was that the glutamate-bound and AMPA-bound proteins tended to form needle crystals at mildly basic pH, while the kainate-bound S1S2 formed plate and three-dimensional crystals under

mildly acidic conditions. The reasons for the differences in crystal morphology are unclear. However, the difference in crystallization behavior is probably due to the three-dimensional shape and surface of the protein-ligand complexes rather than to the properties of the ligand since the structural differences between glutamate and AMPA are more than those between glutamate and kainate. In other words, different S1S2-ligand complexes may have distinct protein conformations and/or surface characters. This difference in crystallization behavior between the glutamate, AMPA, and kainate complexes is particularly interesting in the light of the fact that glutamate and AMPA produce desensitizing currents while kainate produces nondesensitizing currents in the intact receptor (Mano et al., 1996).

In conclusion, limited proteolysis analyzed by Maldi-MS and N-terminal sequencing, deletion mutagenesis, and multiple sequence alignment provided powerful approaches to elucidate the minimal functional ligand binding domain of the GluR2 receptor for biochemical, structural, and pharmaceutical studies. S1S2I was more thermally stable, more protease-resistant, and produced much better crystals than S1S2 and should therefore facilitate molecular-level studies of AMPA-sensitive GluR2 receptors. The knowledge of design, analysis, large-scale production, and crystallization of stable constructs of the GluR2 ligand binding domain may be applied to other iGluRs.

Materials and methods

Materials

Plasmid pHS1S2 (Chen & Gouaux, 1997) was the template for PCR or the parent plasmid for cassette mutagenesis in the construction of the other variants. HPLC-purified oligonucleotides were purchased from Operon (Alameda, California) and used as PCR primers or cassette inserts after phosphorylation. They are PRMA1, CGGAATTCGCCATGGTTGTCACCCTAACT; PRMA2, TGGCAATTTCTGCAGCTAAG; INSB1, CATGGAA AACAAAACTGTGGTG; INSB2, GTGACCACCACAGTTTT GTTTTC; PRMC1, GAGTAGCCAGAGTCCGG; PRMC2, GCC CAAGCTTCTCGAGTCAGCTGCCGCACTCTCCTTTG; PRM1, GGGCTACTGTGTTGACTT; PRM4, CTTCTGCGGTAGTCC TC; PRMD2, ATCCAGAGGGCCACCTTTCTTGGACTTCTGA GGCTT; PRMD3, AAAGGTGGCCCTCTGGATGGTACTGAG AGGATGGTGTCTCC; PRME2, GTTACCATCAGTGCCTTTG GACTTCTGAGGCTT; PRME3, GGCACTGATGGTAACCCCA TCGAAAGTGCTGA; PRMF2, GTTACCATCAGTGCCAGGC TTCTTGATCATGATAG; PRMF3, GGCACTGATGGTAACGA GAGGATGGTGTCTCC; PRMG2, ATCCAGAGGGCCACCTT TAGGCTTCTTGATCATGATAG; PRMG3, AAAGGTGGCCC TCTGGATGGTACTCCCATCGAAAGTGCTGA; PRMJ2, GTT ACCATCAGTGCCAAGACTCATGAAGGGCTT; and PRMJ3, GGCACTGATGGTAACATTGCTTATGGAACATTAGAC. Other reagents and supplies have been previously described (Chen & Gouaux, 1997).

Buffers

Buffer 1, 20 mM Tris-HCl, 10 mM $CaCl_2$, 100 mM NaCl, pH 8.0. Buffer 2, 20 mM Tris-HCl, 200 mM NaCl, 1 mM EDTA, pH 7.4. Buffer 3, 20 mM Tris-HCl, pH 8.5, 250 mM NaCl, 10 mM KCl, 1 mM EDTA, 0.05% PEG 3350. Buffer 4, 30 mM Tris-HCl, pH 7.2, 100 mM KSCN, 2.5 mM $CaCl_2$, 10% glycerol. Buffer 5, 50 mM Tris-HCl, 1 mM EDTA, 100 mM NaCl, pH 8.0. Buffer 6, 50 mM Tris-HCl, 10 mM EDTA, 100 mM NaCl, 0.5% Triton X-100, pH 8.0. Buffer 7, 50 mM Tris-HCl, pH 7.4, 5 mM EDTA, 8 M guanidine hydrochloride, 50 mM DTT. Buffer 8, 20 mM NaOAc, 4 M guanidine hydrochloride, 1 mM EDTA, 1 mM DTT, pH 4.5. Buffer 9, pH 8.5, 10 mM NaCl, 0.4 mM KCl, 0.65 M arginine-HCl, 1 mM EDTA. Buffer 10A, 10 mM Tris-HCl, 1 mM glutamate, 1 mM EDTA, 1 mM DTT, pH 6.6. Buffer 10B, Buffer 10A supplemented with 1 M NaCl. Buffer 11A, 10 mM HEPES, pH 6.5, 1 mM EDTA. Buffer 11B, Buffer 11A supplemented with 1 M NaCl. Buffer 12A, 10 mM NaOAc, pH 5.5, 1 mM EDTA, 1 mM glutamate. Buffer 12B, Buffer 12A supplemented with 500 mM NaCl.

Plasmid construction

PCR reactions (100 μL) contained 0.02 nM template, 200 nM of each primer, 200 μM dNTPs, and 0.037 U/μL *Pfu* DNA polymerase. The PCR mixture was heated at 94 °C for 5 min before the thermal cycles began (94 °C, 45 s/52 °C, 45 s/ 72 °C, 60 s; 25 cycles). Primers PRMA1 and PRMA2 were used to generate the gene fragment with the additional N-terminal sequences for HS1S2A. The PCR product was subcloned into pHS1S2 using Nco I and Pst I sites, resulting in plasmid pHS1S2A. Plasmid pHS1S2B was constructed by insertion of the gene fragment between Nco I and BstE II sites using the phosphorylated oligos of INSB1 and INSB2. Phosphorylation was performed as described (Chen & Gouaux, 1996). Plasmid pHS1S2C were constructed by a PCR using primers PRMC1 and PRMC2 and a subcloning step using BamH I and Xho I sites. Plasmids pHS1S2X (X = D, E, F, G, H, or J) was constructed by three PCRs followed by a subcloning step using Pst I and Bgl II sites. The first PCR produced mutations at the C-terminus of S1 and in the linker section using PRM1 and PRMX2, and the second PCR generated mutations in the linker section and at the N-terminus of S2 using PRMX3 and PRM4 primers. The products from the first two PCRs served as the template for the third PCR using PRM1 and PRM4 primers to generate the full-length insert for subcloning. Plasmid pHS1S2I was constructed by subcloning the insert between Bgl II and Xho I from pHS1S2C into pHS1S2H.

Protein expression, purification, folding, and ligand binding assay

Expression and purification of the HS1S2 mutants were performed according to the methods worked out for HS1S2 (Chen & Gouaux, 1997). The folding reactions were carried out as follows. The FPLC-purified protein (0.5 mg/mL, 200 μL) was dialyzed against 20 volumes of the folding buffer, then 20 volumes of Buffer 4 using MWCO 25-kD membranes at 4 °C overnight. The dialyzed folding reaction mixture was centrifuged at 40,000 rpm (TL 100, Beckman) for 1 h. The supernatant was analyzed by SDS-PAGE to estimate the total amounts of the solubilized protein. For the ligand binding assay, GSWP 02500 membranes (Chen & Gouaux, 1997) were used and the binding reaction mixture with a total volume of 500 μL contained 20 nM [^{3}H]-AMPA (10.6 Ci/mmol) and 10 μL of the centrifuged refolding mixture.

Large scale protein production

An overnight culture of *E. coli* BL21(DE3) cells transformed with plasmid pHS1S2 or pHS1S2I (100 mL) was added to fresh LB_{kan}

media (LB media supplemented with 30 μg/mL kanamycin, 10 L) and the cell growth proceeded at 37 °C for 3 h. IPTG was then added to a final concentration of 1 mM and the culture was incubated for an additional 2 h. The induced cells were collected by centrifugation at 4,000 rpm for 20 min and resuspended in 100 mL of Buffer 5 with 100 mg of lysozyme, 120 mg of deoxycholic acid, 1 mg of DNase I and 100 μL of 1 M PMSF. After breaking the cells with a French Press, the suspension was centrifuged at 17,000 rpm for 30 min, yielding the crude inclusion bodies. The crude inclusion bodies were washed with 200 mL of Buffer 6 supplemented with 1 mM PMSF and then with Buffer 2 containing 1 mM PMSF. The washed inclusion bodies from the 10 L culture were solubilized in 90 mL of Buffer 7 at room temperature for 4 h. The solubilization solution was centrifuged at 40,000 rpm at 20 °C for 1 h and the supernatant was diluted with 500 mL of Buffer 8. The diluted solution was stirred at 4 °C for 1 h and centrifuged at 40,000 rpm at 4 °C for an additional hour. Prior to folding, the protein concentration was adjusted with cold Buffer 8 to 1–1.5 mg/mL. The solubilized protein was dialyzed against 25 volumes of Buffer 3 for HS1S2 or Buffer 9 for HS1S2I at 4 °C (2 × 8 h). Next, the solubilized protein was separated from the precipitate by centrifugation (35,000 rpm, 1 h). The supernatant was treated with GSH/GSSG (1 mM/0.2 mM) at 4 °C overnight and concentrated about 30-fold using an Amicon concentrator. The concentrated folding reaction mixture was filtered (0.22 μm) and loaded onto a XK 26/100 Superose 12 column in Buffer 2 supplemented with 1 mM glutamate. The flow rate was 2 mL/min. The peak corresponding to the monomer was collected and the protein was stored at −80 °C.

Preparative thrombin digestion of HS1S2 and purification of S1S2

The concentration of purified monomeric HS1S2 was adjusted to 2 mg/mL in Buffer 2 supplemented with 10 mM glutamate and 5 mM $CaCl_2$. Thrombin was solubilized in the reaction buffer to make a 50 U/mL solution and 2.5 U of thrombin per milligram of HS1S2 were added to the protein solution. The digestion reaction mixture was kept at 4 °C overnight. The next day, EDTA (10 mM), and PMSF (1 mM) were added and the reaction mixture was kept at room temperature for 15 min. The reaction mixture was dialyzed against 60 volumes of Buffer 10A and purified on a Q-Sepharose column (5 mL of resin, Buffer 10A and Buffer 10B, flow rate 0.5 mL/min). The peak fractions were collected and dialyzed against Buffer 11A and further purified on a 5-mL Hitrap Q column (Buffer 11A and Buffer 11B, 2 mL/min).

Preparative trypsin digestion of HS1S2I and purification of S1S2I

Into the purified HS1S2I solution $CaCl_2$ (10 mM) and trypsin (1:1,500, trypsin: HS1S2I, w/w) were added and the solution was mixed thoroughly. The cleavage reaction was carried out at room temperature for 40 min. Afterward, EDTA and PMSF were added to final concentrations of 20 and 1.3 mM, respectively, and the mixture was shaken for 5 min. The same amount of PMSF was added again and the solution was shaken for another 5 min and then placed on ice. After dialysis against Buffer 12A, S1S2I was purified on a 5-mL Hitrap SP column (Buffer 12A and Buffer 12B, 1 mL/min).

Preparation of SeMet S1S2I

E. coli B834(DE3) cells transformed with pS1S2I and grown overnight in 100 mL of M9 media (Yang et al., 1990) supplemented with 5% LB media were collected by centrifugation at 4,000 rpm (4 °C, 5 min). The cells were resuspended in 10 L of M9 media and incubated at 37 °C until the OD_{600} reached 0.8 (about 10 h). IPTG was added to 1 mM and the cells were collected after 3 h of induction. Purification, folding, and trypsin digestion of SeMet HS1S2I and purification of SeMet S1S2I were carried out according to HS1S2I and S1S2I protocols except that all of the buffers were degassed and 5 mM β-mercaptoethanol was included in the folding and purification buffers.

Trypsin digestion of HS1S2 in the presence (Glu^+) and absence (Glu^-) of glutamate

Glu^- HS1S2 was prepared by dialyzing the purified monomeric protein solution against 100 volumes of Buffer 2 with six buffer changes at 4 °C. Glu^+ HS1S2 was prepared by addition of glutamate (2 mM, final concentration) to Glu^- HS1S2. The reaction mixture (200 μL) contained 60 μg of protein and 0.8 μg of trypsin in Buffer 1. The reaction was carried out at room temperature for different periods of time. At each time point, 28 μL of the reaction mixture was withdrawn, treated with PMSF and analyzed by SDS-PAGE.

Limited proteolysis of HS1S2 and Maldi-MS analysis

Trial protease digestion reactions (100 μL) were carried out at room temperature for 30 min using final protease concentrations of 10^{-6}–10^{-3} U/mL and a protein concentration of 0.2 mg/mL in Buffer 1. The reactions were stopped by addition of EDTA (12.5 mM) and diisopropyl fluorophosphate (50 mM) followed by incubation at room temperature for 10 min. The reaction mixture was analyzed by SDS-PAGE. Optimal conditions determined from the trial digestion were used to prepare samples for Maldi-MS experiments (Columbia University, New York). The Maldi-MS data were analyzed using GPMAW software (WindowChem Software, Fairfield, California).

Crystallization of S1S2 and S1S2I

The hanging drops (2 mL for screening and 4–10 mL for preparative crystallization) were prepared by mixing equal volumes of the protein stock solution (7.5 and 15 mg/mL) and the reservoir solution (500 mL). Crystallization screens of S1S2 and S1S2I in the presence or absence of different ligands (glutamate, kainate, or AMPA) employed the Hampton Crystal Screen Kit, the ammonium sulfate-pH, the PEG 6000-pH, and the MPD-pH Grid Kits. Conditions that gave microcrystals were refined by changing the pH, PEG, and salt concentrations. Crystal seeding was performed according to previously described methods (Stura & Wilson, 1990). The details of the crystallization conditions are described in Results. The space group and unit cell dimensions of the S1S2I complex were determined by screened precession photographs and by indexed oscillation images collected on X-ray film and on a R-Axis II area detector, respectively.

Acknowledgments

Drs. Hirsh, Hendrickson, Thanos, Palmer, Pyle, Karlin, and Javitch, and their laboratories are acknowledged for their helpful assistance and for

equipment use. We also thank Ms Gawinowicz and the Protein Core facility at Columbia University for the Maldi-MS analysis. Support for this research was provided in part by a Searle Scholar Award, an NSF Young Investigator Award, and an Alfred P. Sloan Research Fellowship (E.G.).

References

Arvola M, Keinänen K. 1996. Characterization of the ligand-binding domains of glutamate receptor (GluR)-B and GluR-D subunits expressed in *Escherichia coli* as periplasmic proteins. *J Biol Chem 271*:15527–15532.

Bennett JA, Dingledine R. 1995. Topology profile for a glutamate receptor: Three transmembrane domains and a channel-lining reentrant membrane loop. *Neuron 14*:373–384.

Bettler B, Boulter J, Hermans-Borgmeyer I, O'Shea-Greenfield A, Deneris ES, Moll C, Borgmeyer U, Hollmann M, Heinemann S. 1990. Cloning of a novel glutamate receptor subunit, GluR5: Expression in the nervous system during development. *Neuron 5*:583–595.

Chen GQ, Gouaux E. 1997. Overexpression of a glutamate receptor (GluR2) ligand binding domain in *Escherichia coli*: Application of a novel protein folding screen. *Proc Natl Acad Sci USA 94*:13431–13436.

Chen GQ, Gouaux JE. 1996. Overexpression of bacterio-opsin in *Escherichia coli* as a fusion to maltose binding protein: Efficient regeneration and cleavage with trypsin. *Protein Sci 5*:456–467.

Cohen SL. 1996. Domain elucidation by mass spectrometry. *Structure 4*:1013–1016.

Cohen SL, Ferré-D'Amaré AR, Burley SK, Chait BT. 1995. Probing the solution structure of the DNA-binding protein Max by a combination of proteolysis and mass spectroscopy. *Protein Sci 4*:1088–1099.

Dingledine R, Hume RI, Heinemann SF. 1992. Structural determinants of barium permeation and rectification in non-NMDA glutamate receptor channels. *J Neurosci 12*:4080–4087.

Ferrer-Montiel AV, Sun W, Montal M. 1996. A single tryptophan on M2 of glutamate receptor channels confers high permeability to divalent cations. *Biophysical J 71*:749–758.

Hollmann M, Heinemann S. 1994. Cloned glutamate receptors. *Annu Rev Neurosci 17*:31–108.

Hollmann M, Maron C, Heinemann S. 1994. N-Glycosylation site tagging suggests a three transmembrane domain topology for the glutamate receptor GluR1. *Neuron 13*:1331–1343.

Hume RI, Dingledine R, Heinemann SF. 1991. Identification of a site in glutamate receptor subunits that controls calcium permeability. *Science 253*:1028–1031.

Jancarik J, Kim S-H. 1991. Sparse matrix sampling: A screening method for crystallization of proteins. *J Appl Cryst 24*:409–411.

Keinänen K, Jouppila A, Kuusinen A. 1998. Characterization of the kainate-binding domain of the glutamate receptor GluR-6 subunit. *Biochem J 330*:1461–1467.

Keinänen K, Köhr G, Seeburg PH, Laukkanen M-L, Oker-Blom C. 1994. High-level expression of functional glutamate receptor channels in insect cells. *Bio Technology 12*:802–806.

Kuryatov A, Laube B, Betz H, Kuhse J. 1994. Mutational analysis of the glycine-binding site of the NMDA receptor: Structural similarity with bacterial amino acid-binding proteins. *Neuron 12*:1291–1300.

Kuusinen A, Arvola M, Keinänen K. 1995a. Molecular dissection of the agonist binding site of an AMPA receptor. *EMBO J 14*:6327–6332.

Kuusinen A, Arvola M, Oker-Blom C, Keinänen K. 1995b. Purification of recombinant GluR-D glutamate receptor produced in Sf21 insect cells. *Eur J Biochem 233*:720–726.

Laube B, Kuhse J, Betz H. 1998. Evidence for a tetrameric structure of recombinant NMDA receptors. *J Neurosci 18*:2954–2961.

Liljas A, Kannan KK, Bergsten PC, Waara I, Fridborg K, Strandberg B, Carlbom U, Jarup L, Lovgren S, Petef M. 1972. Crystal structure of human carbonic anhydrase C. *Nat New Biol 235*:131–137.

Mano I, Lamed Y, Teichberg VI. 1996. A Venus flytrap mechanism for activation and desensitization of α-amino-3-hydroxy-5-methyl-4-isoxazole propionic acid receptors. *J Biol Chem 271*:15299–15302.

Mano I, Teichberg VI. 1998. A tetrameric subunit stoichiometry for a glutamate receptor-channel complex. *NeuroReport 9*:327–331.

Mori H, Mishina M. 1995. Structure and function of the NMDA receptor channel. *Neuropharmacology 34*:1219–1237.

Nagi AD, Regan L. 1997. An inverse correlation between loop length and stability in a four-helix-bundle protein. *Fold Design 2*:67–75.

Nakanishi N, Shneider NA, Axel R. 1990. A family of glutamate receptor genes: Evidence for the formation of heteromultimeric receptors with distinct channel properties. *Neuron 5*:569–581.

Nakanishi S, Masu M. 1994. Molecular diversity and functions of glutamate receptors. *Annu Rev Biophys Biomol Struct 23*:319–348.

O'Hara PJ, Sheppard PO, Thøgersen H, Venezia D, Haldeman BA, McGrane V, Houamed KM, Thomsen C, Gilbert TL, Mulvihill ER. 1993. The ligand-binding domain in metabotropic glutamate receptors is related to bacterial periplasmic binding proteins. *Neuron 11*:41–52.

Paas Y, Devillers-Thiéry A, Changeux J-P, Medevielle F, Teichberg VI. 1996. Identification of an extracellular motif involved in the binding of guanine nucleotides by a glutamate receptor. *EMBO J 15*:1548–1556.

Reeke GNJ, Becker JW, Edelman GM. 1975. The covalent and three-dimensional structure of concanavalin A. IV. Atomic coordinates, hydrogen bonding, and quaternary structure. *J Biol Chem 250*:1525–1547.

Rogers J, Early P, Carter C, Calame K, Bond M, Hood L, Wall R. 1980. Two mRNAs with different 3′ ends encode membrane-bound and secreted forms of immunoglobulin μ chain. *Cell 20*:303–312.

Rosenmund C, Stern-Bach Y, Stevens CF. 1998. The tetrameric structure of a glutamate receptor channel. *Science 280*:1596–1599.

Seeburg PH. 1993. The *TINS/TiPS* lecture. The molecular biology of mammalian glutamate receptor channels. *Trends Neurosci 16*:359–365.

Sibanda BL, Blundell TL, Thornton JM. 1989. Conformation of β-hairpins in protein structures. A systematic classification with applications to modeling by homology, electron density fitting and protein engineering. *J Mol Biol 206*:759–777.

Stern-Bach Y, Bettler B, Hartley M, Sheppard PO, O'Hara PJ, Heinemann SF. 1994. Agonist selectivity of glutamate receptors is specified by two domains structurally related to bacterial amino acid-binding proteins. *Neuron 13*:1345–1357.

Stura EA, Wilson IA. 1990. Analytical and production seeding techniques. *Method Enzymol 1*:38–49.

Sutcliffe MJ, Wo ZG, Oswald RE. 1996. Three-dimensional models of non-NMDA glutamate receptors. *Biophysical J 70*:1575–1589.

Tam R, Saier MH. 1993. Structural, functional, and evolutionary relationships among extracellular solute-binding receptors of bacteria. *Microbiol Rev 57*:320–346.

Verdoorn TA, Burnashev N, Monyer H, Seeburg PH, Sakmann. 1991. Structural determinants of ion flow through recombinant glutamate receptor channels. *Science 252*:1715–1718.

Watkins JC, Krogsgaard-Larsen P, Honoré T. 1990. Structure-activity relationships in the development of excitatory amino acid receptor agonists and competitive antagonists. *Trends Pharmacol Sci 11*:25–33.

Wo ZG, Oswald RE. 1994. Transmembrane topology of two kainate receptor subunits revealed by N-glycosylation. *Proc Natl Acad Sci USA 91*:7154–7158.

Wo ZG, Oswald RE. 1995. Unraveling the modular design of glutamate-gated ion channels. *Trends Neurosci 18*:161–168.

Wo ZG, Oswald RE. 1996. Ligand-binding characteristics and related structural features of the expressed goldfish kainate receptors: Identification of a conserved disulfide bond and three residues important for ligand binding. *Mol Pharmacol 50*:770–780.

Yang W, Hendrickson WA, Kalman ET, Crouch RJ. 1990. Expression, purification and crystallization of natural and selenomethionly recombinant ribonuclease H from *Escherichia coli*. *J Biol Chem 265*:13553–13559.